Bioorganic & Medicinal Chemistry 22 (2014) 6552–6563

Contents lists available at ScienceDirect

Bioorganic & Medicinal Chemistry

journal homepage: www.elsevier.com/locate/bmc

An efficient synthesis and biological screening of benzofuran and benzo[*d*]isothiazole derivatives for *Mycobacterium tuberculosis* DNA GyrB inhibition

Kummetha Indrasena Reddy [b], Konduri Srihari [b], Janupally Renuka [a], Komanduri Shruthi Sree [a], Aruna Chuppala [b], Variam Ullas Jeankumar [a], Jonnalagadda Padma Sridevi [a], Kondra Sudhakar Babu [b,*], Perumal Yogeeswari [a], Dharmarajan Sriram [a,*]

[a] *Department of Pharmacy, Birla Institute of Technology & Science-Pilani, Hyderabad Campus, Jawaharnagar, Shameerpet, Hyderabad 500078, India*
[b] *Department of Chemistry, Sri Krishnadevaraya University, Anantapur 515055, India*

ARTICLE INFO

Article history:
Received 26 August 2014
Revised 10 October 2014
Accepted 14 October 2014
Available online 18 October 2014

Keywords:
Tuberculosis
Antitubercular
DNA gyrase
Benzofuran
Benzo[*d*]isothiazole
Cytotoxicity

ABSTRACT

A series of twenty eight molecules of ethyl 5-(piperazin-1-yl)benzofuran-2-carboxylate and 3-(piperazin-1-yl)benzo[*d*]isothiazole were designed by molecular hybridization of thiazole aminopiperidine core and carbamide side chain in eight steps and were screened for their in vitro *Mycobacterium smegmatis* (MS) GyrB ATPase assay, *Mycobacterium tuberculosis* (MTB) DNA gyrase super coiling assay, antitubercular activity, cytotoxicity and protein–inhibitor interaction assay through differential scanning fluorimetry. Also the orientation and the ligand–protein interactions of the top hit molecules with MS DNA gyrase B subunit active site were investigated applying extra precision mode (XP) of Glide. Among the compounds studied, 4-(benzo[*d*]isothiazol-3-yl)-*N*-(4-chlorophenyl)piperazine-1-carboxamide (**26**) was found to be the most promising inhibitor with an MS GyrB IC_{50} of 1.77 ± 0.23 μM, 0.42 ± 0.23 against MTB DNA gyrase, MTB MIC of 3.64 μM, and was not cytotoxic in eukaryotic cells at 100 μM. Moreover the interaction of protein–ligand complex was stable and showed a positive shift of 3.5 °C in differential scanning fluorimetric evaluations.

1. Introduction

Tuberculosis continues to be a global threat with highest morbidity and mortality rates worldwide, killing approximately 1.3 million in 2012.[1] Mycobacterial infections remain to be the largest cause of death worldwide.[2] Furthermore, rapid emergence of extensive drug-resistant tuberculosis (XDR-TB) and multidrug-resistant tuberculosis (MDR-TB) are a major concern with currently used first-line TB drugs which are 40 years old and second-line drugs possessing variable efficacy and serious side effects.[1] Hence design of new inhibitors with novel mechanisms of action, greater efficacy against mycobacterial enzymes that aid in newer combination regimens for treating MDR-TB and XDR-TB are in urgent need.[3,4] In general, bacterial type II topoisomerases (DNA gyrase and DNA topoisomerase IV) are clinically proven as antibacterial targets, while *Mycobacterium tuberculosis* (MTB) is unusual in that it possess only one type II topoisomerase that is DNA gyrase.[5] Though the main function is to supercoil DNA, it also shows enhanced relaxation, DNA cleavage, and decatenation activities.[6] DNA gyrase is a heterotetramer with two subunits, gyrase A (GyrA) and gyrase B (GyrB), that together form a functional heterodimer structure A2B2. While the GyrA subunit is primarily involved in the breakage and reunion of the bacterial DNA, subsequently the GyrB subunit possesses an ATP-ase activity.[7] While the GyrA subunit has been well understood with most of the fluoroquinolones targeting it but not much has been explored on the GyrB subunit except one approved antibiotic, novobiocin that has been withdrawn from the market due to severe safety concern and poor pharmacological properties.[8] Moreover, GyrB has been genetically demonstrated to be a bactericidal drug target in MTB, but till date there have not been any effective therapeutics developed against this target for TB which was why we made an attempt toward synthesis of a chemical class of molecules targeting the GyrB subunit.[9] In this study we disclose two novel classes of mycobacterial DNA gyrase B inhibitors developed via molecular hybridization of earlier reported GyrB leads. The designed molecules were subsequently synthesized and evaluated in vitro for their ability to inhibit DNA gyrase B enzyme and whole cell MTB as steps toward the derivation of structure–activity relationship.

* Corresponding authors. Tel.: +91 40663030506; fax: +91 4066303998 (D. S.).
E-mail address: dsriram@hyderabad.bits-pilani.ac.in (D. Sriram).

http://dx.doi.org/10.1016/j.bmc.2014.10.016
0968-0896/

The thermal stability of the protein with the most potent ligand was also ascertained biophysically through differential scanning fluorimetry experiment.

2. Results and discussion

2.1. Design and synthesis

Information on the common properties of the binding groups is essential for resolving the type of inhibitor binding to the target protein. We had previously designed and developed various classes of inhibitors as mycobacterial GyrB inhibitors utilizing the concept of molecular hybridization.[8] The preliminary structure–activity profiling studies of these leads provided valuable information regarding the basic structural requirements for achieving selective inhibition of mycobacterium GyrB. An imperative from our previous research efforts revealed the importance of hydrophobic interactions in bringing specificity toward the mycobacterial GyrB protein. These findings were equally supported by the crystallographic characterization of the aminopyrazinamide analogs to GyrB protein by researchers from AstraZeneca and reported that the presence of a unique hydrophobic pocket in the active site brought specificity toward the mycobacterial GyrB protein. Having understood the important structural requisite for bringing about specificity and potency toward the mycobacterial GyrB domain, we envisaged re-engineering of the previously reported leads (compounds **1**, **2** and **3** in Fig. 1) to deliver a novel scaffold/lead with better antimycobacterial activity via inhibition of the gyrase domain. The design strategy utilized for developing the inhibitor has been sketched in Figure 1. Optimization of the structural classes was guided by two main criteria (i) to enhance hydrophobicity of the molecule so as to facilitate affinity toward the GyrB domain and (ii) to evaluate steric and electronic effects that could enhance the antimycobacterial potency. Chemical structure of previously reported synthetic inhibitors of DNA GyrB bearing a benzofuran core (**1**),[10] urea side chain (**2**–**3**)[11] were selected for the design of novel inhibitors through molecular hybridization (Series 1 and 2).

In our effort, starting from previously reported GyrB inhibitors, optimization at the left hand core was conducted simultaneously by two approaches. In the first approach we retained a more hydrophobic benzofuran nucleus was employed (compound **1**) and in the second approach, we introduced an isothiazole group in place of benzofuran core. Overall, a rationalized effort to enhance the hydrophobicity of the lead molecule to facilitate the affinity toward the GyrB domain was attempted. On the right hand core, various urea and thiourea derivatives were introduced in both the series to increase stability and also to explore the steric and electronic effects on the antimycobacterial potency. An additional optimization strategy was the replacement of the *N*-linked aminopiperidine between the LHS and the RHS groups with a piperazine core. Thus a set of twelve compounds in each series were designed and synthesized and as presented in Tables 1 and 2.

The designed ligands (Series 1 and 2) were constructed by a simple and straightforward strategy as shown in Schemes 1 and 2. To prepare benzofuran based leads (compounds **9**–**22**), the ligands were assembled by following the protocol depicted in Scheme 1. Scaffold ethyl 5-(piperazin-1-yl)benzofuran-2-carboxylate (**8**) was prepared by reported procedure,[10] in brief synthesis began by nitrating the salicylaldehyde (**4**). The so obtained 2-hydroxy-5-nitrobenzaldehyde (**4**) on subsequent treatment with ethyl bromoacetate in presence of sodium carbonate in *N*-methyl pyrrolidine gave ethyl 5-nitrobenzofuran-2-carboxylate in good yields and purity. Subsequent reduction of the nitro group at the 5th position of the benzofuran core gave the corresponding ethyl 5-aminobenzofuran-2-carboxylate (**7**) in excellent yields. This (**7**) on further alkylation with bis-(2-chloroethyl)amine using sodium carbonate as base in 1-propanol gave the scaffold **8**. The final library (**9**–**22**) was then assembled by coupling the so obtained ethyl 5-(piperazin-1-yl)benzofuran-2-carboxylate (**8**) with various commercially available isocyanates and thiocyanates as depicted in Table 1.

The synthetic strategy followed for developing the Series 2 (**25**–**38**) has been sketched in Scheme 2. As depicted, synthesis started with alkylation of commercially available 3-chloro-1, 2-benzisothiazole with piperazine in refluxing ethanol, to give 3-(piperazin-1-yl)benzo[*d*]isothiazole in good yields. The dialkylated side product was countered by adding excess of piperazine. The final library (**25**–**38**) was then generated by coupling the so obtained 3-(piperazin-1-yl)benzo[*d*]isothiazole with various commercially available isocyanates and thiocyanates as depicted in Table 2.

2.2. Pharmacological evaluation

ATPase assay was done using *Mycobacterium smegmatis* (MS) GyrB protein, which was cloned into a prokaryotic expression

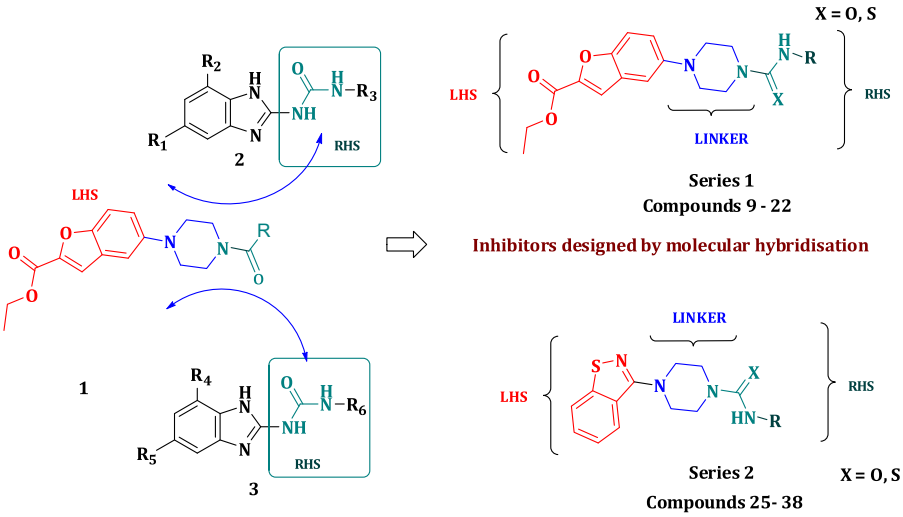

Figure 1. Strategy employed for designing the lead.

Table 1
In vitro evaluation of the synthesized derivatives

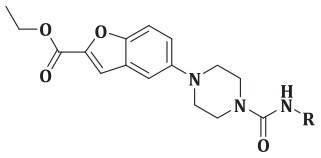

Compound 9-15

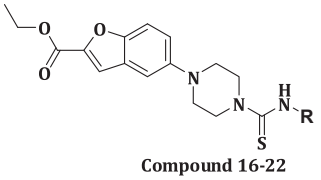

Compound 16-22

Compd	R	MS GyrB assay (IC_{50}) (μM)	MTB supercoiling assay (IC_{50}) (μM)	MTB MIC (μM)	Cytotoxicity (% inhib.)
9	Phenyl	16.89 ± 0.33	7.14 ± 0.48	92.62	21.30
10	4-Chlorophenyl	20.67 ± 0.55	18.2 ± 0.18	16.76	19.23
11	4-Acetylphenyl	7.86 ± 0.26	3.55 ± 0.33	83.54	21.63
12	4-Nitrophenyl	5.07 ± 0.44	2.93 ± 0.31	16.30	19.57
13	4-Methoxyphenyl	8.19 ± 0.33	7.33 ± 0.71	4.24	19.90
14	Benzyl	4.32 ± 0.21	3.12 ± 0.25	35.46	40.87
15	4-Chlorobenzyl	2.97 ± 0.12	1.61 ± 0.18	64.61	21.60
16	Phenyl	15.63 ± 0.74	7.2 ± 0.35	35.26	22.89
17	4-Chlorophenyl	35.18 ± 0.41	13.24 ± 0.22	16.06	29.98
18	4-Acetylphenyl	27.34 ± 1.32	16.9 ± 1.56	31.52	21.19
19	4-Nitrophenyl	12.91 ± 0.74	10.55 ± 0.11	62.57	25.82
20	4-Methoxyphenyl	24.39 ± 0.82	19.8 ± 0.77	16.25	20.65
21	Benzyl	20.45 ± 0.88	9.1 ± 0.34	33.91	45.84
22	4-Chlorobenzyl	29.90 ± 0.62	11.25 ± 0.51	62.03	41.48
Novobiocin		180 ± 3.9 nM	46 ± 10 nM	nd	nd
Isoniazid		nd	nd	0.66	nd
Rifampicin		nd	nd	0.23	nd
Ofloxacin		nd	nd	2.16	nd
Ethambutol		nd	nd	0.66	nd

Nd indicates not determined.

Table 2
In vitro evaluation of the synthesized derivatives

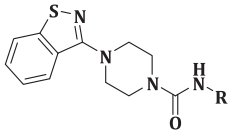

Compounds 25-31

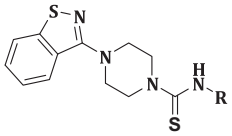

Compounds 32-38

Compd	R	MS GyrB assay (IC_{50}) (μM)	MTB supercoiling assay (IC_{50}) (μM)	MTB MIC (μM)	Cytotoxicity (% inhib.)
25	Phenyl	19.87 ± 0.77	4.59 ± 0.24	68.92	26.99
26	4-Chlorophenyl	1.77 ± 0.14	0.42 ± 0.23	3.44	20.29
27	4-Acetylphenyl	29.3 ± 0.92	9.51 ± 0.21	28.70	20.18
28	4-Nitrophenyl	27.11 ± 0.64	12.2 ± 0.66	28.51	20.86
29	4-Methoxyphenyl	26.18 ± 0.63	12.2 ± 0.31	14.72	37.62
30	Benzyl	2.36 ± 0.31	1.18 ± 0.23	1.9	30.2
31	4-Chlorobenzyl	6.88 ± 0.35	3.55 ± 0.17	14.1	29.08
32	Phenyl	9.14 ± 0.38	3.9 ± 0.62	15.22	39.28
33	4-Chlorophenyl	9.32 ± 0.26	4.21 ± 0.26	3.51	44.18
34	4-Acetylphenyl	11.09 ± 0.43	8.4 ± 0.45	13.82	40.70
35	4-Nitrophenyl	1.81 ± 0.24	0.83 ± 0.19	13.72	27.56
36	4-Methoxyphenyl	2.86 ± 0.21	1.05 ± 0.31	3.54	18.99
37	Benzyl	45.97	>25	14.72	19.06
38	4-Chlorobenzyl	11.32 ± 0.55	4.4 ± 0.41	6.82	25.94
Novobiocin		180 ± 3.9 nM	46 ± 10 nM	nd	nd
Isoniazid		nd	nd	0.66	nd
Rifampicin		nd	nd	0.23	nd
Ofloxacin		nd	nd	2.16	nd
Ethambutol		nd	nd	0.66	nd

Nd indicates not determined.

vector pQE2 and expressed in BL21 (DE3) pLysS cells. The expressed protein was further induced with a final concentration of 0.1 mM IPTG (isopropyl-β-D-thiogalactopyranoside), purified using Ni-NTA column and further identified by 10% SDS–PAGE. All the synthesized compounds were biologically evaluated for their in vitro MS GyrB ATPase assay. All the twenty eight compounds showed more than 75% of inhibition at 200 μM, and on further testing at concentrations of 100 and 50 μM, thirteen compounds was found to exhibit inhibition more than 60%. Further the compounds **11**, **12**, **13**, **14**, **15**, **19**, **26**, **30**, **31**, **32**, **33**, **35** and **36** were tested at 25, 10, 5, 1 and 0.5 μM concentrations to calculate their IC_{50}s. Compound **26** was found to be the most potent

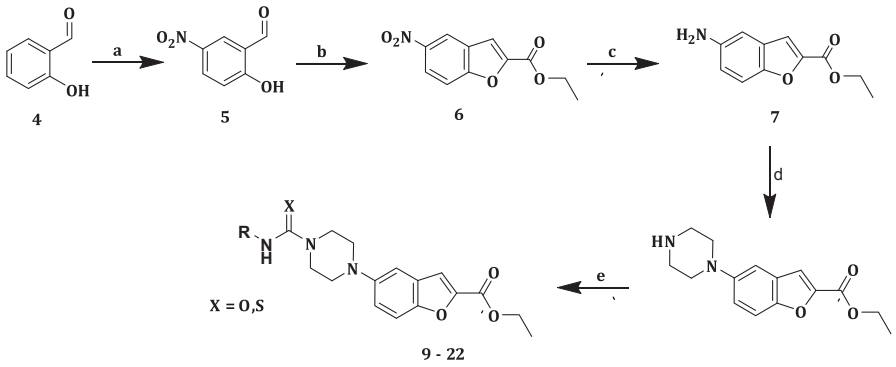

a.HNO_3/AcOH; b.Na_2CO_3,NMP,ethylbromoacetate; c.Raney-Ni, H_2; d. bis-(2-chloro ethyl) amine, sodium carbonate, propanol; e. RNCO/RNCS,TEA, DCM,0°C-rt

Scheme 1. Synthetic protocol adopted to achieve the designed ligands **9**–**22**.

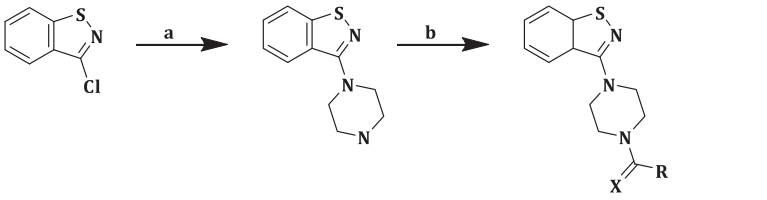

a. piperazine, ethanol, 80°C, b. RNCO/RNCS, TEA, DCM, 0°C-rt

Scheme 2. Synthetic protocol adopted to achieve the designed ligands **25**–**38**.

molecule with an IC_{50} of 1.77 ± 0.14 μM. A dose dependent curve for **26** is shown in Figure 2. As reported previously, ATPase activity was performed using the MS DNA GyrB protein as MTB protein showed less activity. The less activity of MTB was attributed due to its slow growing mechanism when compared to MS.[12] Novobiocin was used as standard inhibitor for the assay, while moxifloxacin was used as a negative control. Brij-35 (detergent) was used to prevent aggregation of molecules during the assay. By performing the assay with MS DNA GyrB protein, we obtained correlation variations approximately 3–5 fold in IC_{50} value between the ATPase activity of MS and the supercoiling activity of MTB. Subsequently this gave us enough confidence to employ MS as a surrogate enzyme to MTB GyrB in the ATPase assay. Furthermore, the other parameters which were considered for using the surrogate MS protein was the sequence homology between MS and MTB gyrase proteins which showed almost 87% identity when performed using BLAST tool, was found to have high degree of conservation in the ATP binding pocket in the two organisms.[13]

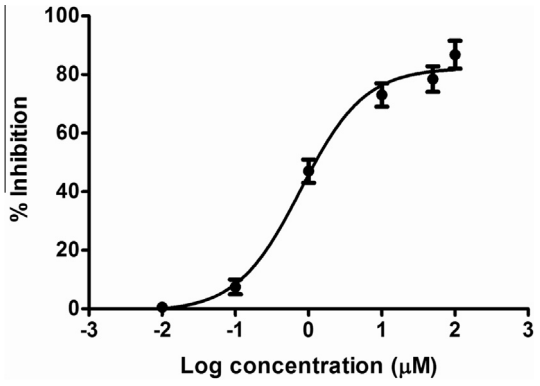

Figure 2. Dose response curve of compound **26** of *Mycobacterium smegmatis* DNA GryB ATPase assay for six different concentrations.

Further to analyze the interaction profile of the molecules based on GyrB assay, we performed molecular docking studies. The molecules were docked into the GyrB ATPase domain of MS retrieved from protein data bank (PDB ID: 4B6C)[12] using extra precision mode (XP) of Glide module in Schrodinger suite (2012).[14] Closer analyses of the co-crystallized ligand (6-(3,4 dimethylphenyl)-3-[[4-[3-(4-methylpiperazin-1 yl)propoxy]phenyl]amino] pyrazine-2-carboxamide) revealed one H-bonding interaction with the amino group of the carboxamide moiety and the oxygen atom of Asp79 residue, while a π-electron bond was observed between the nitrogen atom of piperazine ring and hydrogen atom on the guanidine moiety of Arg82 as shown in Figure 3. Presence of a hydrophobic pocket formed by Val49, Ala53, Ile83, Val97, Val99, Val124, Val128 and Ile171 in which the 3,4-dimethyl phenyl moiety was stabilized by the non-polar interactions with Ile83 and Val128 was also observed. As reported previously, hydrophobic interactions were crucial in bringing selectivity and specificity observed in the enzyme level.[12,13] Upon docking the hit molecules from in vitro GyrB assay, the most potent analog **26** exhibited good docking score of −8.63 kcal/mol with similar orientation to that of the crystal ligand in the active pocket and showed polar contact between oxygen group of ethyl benzofuran-2-carboxylate and Arg141 as illustrated in Figure 4. Secondly, stable interaction was observed between the π-electron environment of thiazole ring of compound **26** and the ammonium ion (NH_3^+) present in the guanidine group of Arg82. The hydrophobic pocket was occupied by the highly hydrophobic 4-chlorophenyl core of (4-chlorophenyl)piperazine-1-carboxamide where it was found to be stabilized by

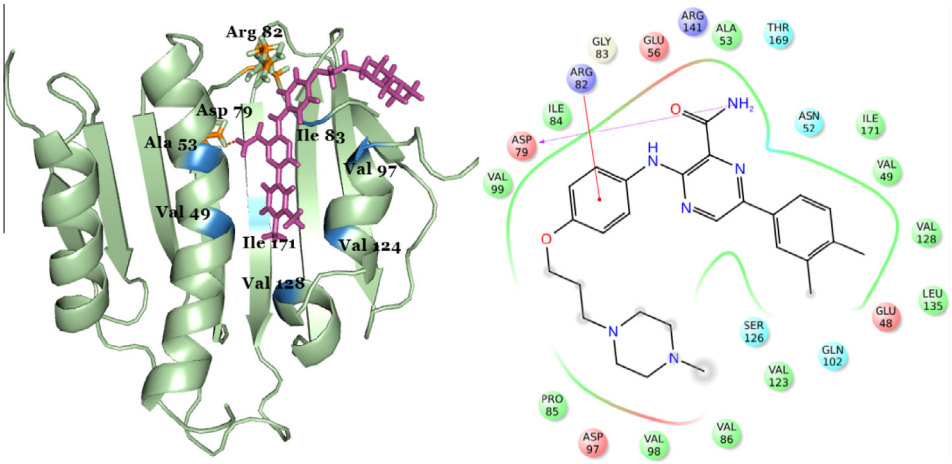

Figure 3. Interaction pattern of the crystal ligand 4B6C (6-(3,4 dimethylphenyl)-3-[[4-[3-(4-methylpiperazin-1 yl)propoxy]phenyl]amino]pyrazine-2-carboxamide) with GyrB ATPase domain of *M. smegmatis*. Hydrophobic pocket is represented by the blue color residues, the polar contacts are shown by the red dotted lines.

non-polar interactions with Val49, Ile 84, Val99, Val123 and Val128. Presence of a halogen group increased the activity as chloro group in the aryl ring resulted in inductive effect which subsequently deactivated the π cloud thereby deactivating the ring. Ultimately, the ring represented as electron acceptor at the proteins active site thereby increasing the affinity toward the active site residues. As previously reported these hydrophobic interactions contributed toward their specificity and bioactivity.[8] All these above illustrations supported the activity of compound **26**. Similarly, compound **25** substituted with a phenyl group showed less docking score of −6.35 kcal/mol when compared to **26** as the removal of the halogen group at 4th position of phenylcarbamoyl moiety drastically reduced the activity. Similarly, substitution of benzyl **30** and 4-chlorobenzyl **31** showed better inhibitory effects with a good docking score of −6.3, −6.1 kcal/mol and in vitro GryB IC_{50} of 2.36 ± 0.31 and 6.88 ± 0.35, respectively. Compounds **28** and **29** with 4-nitro phenyl and 4-methoxy phenyl were observed to be less active (with IC_{50} around 26 μM) displaying poor interactions at the active site with docking scores of −4.2 and −4.5 kcal/mol. Whereas their counter parts, compounds **35** and **36** with thio functional moiety showed 10-fold better activity with IC_{50} around 2 μM. In these compounds, altered binding orientation was observed with the terminal nitro and methoxy groups embedded deep in to the active site pocket with strong hydrophobic interactions. Compound **27** showed the least activity in this series with docking score −3.6 kcal/mol and the 4-acetylphenyl group exhibited no π-electron bonding which made the molecule unstable and disoriented with no hydrophobic interactions as shown in Figure 5. Furthermore, compound **15** (*N*-(4-chlorobenzyl)-4-(benzo[*d*]isothiazol-3-yl)piperazine-1-carboxamide) was found to be equipotent with compound **26** showing polar contact with Asp79 and a π-electron bond between isothiazole ring of benzo[*d*]isothiazole and guanidine moiety of Arg82 similar to that of the crystal ligand as shown in Figure 6 from first series displaying three H-bonds with Asp79, Gly83 and Thr169. Subsequently, the thio substituted 4-chlorobenzyl (**22**) showed lesser activity due to loss of interactions with important amino acid residues. Compound **17** was least active in in vitro MS DNA GyrB activity with less docking score of −3.6 kcal/mol as the molecule aligned in an opposite direction with no polar and hydrophobic contacts within the active site pocket as shown in Figure 7. Overall, benzofuran derivatives, with some exceptions, can be considered as better GyrB inhibitors when compared to benzisothiazole ones. In particular, thio substitution over benzofuran derivatives (compounds **32**–**36** and **38**) can be more preferable as observed from their GyrB activity and MIC values.

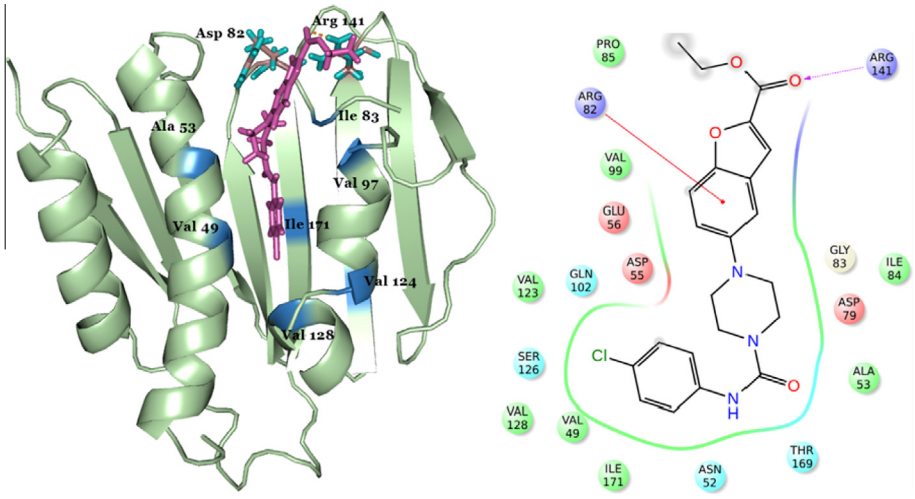

Figure 4. Interaction pattern of the compound **26** (4-(benzo[*d*]isothiazol-3-yl)-*N*-(4-chlorophenyl)piperazine-1-carboxamide) with GyrB ATPase domain of *M. smegmatis*. Hydrophobic pocket is represented by the blue color residues and the polar contacts are shown by the red dotted lines.

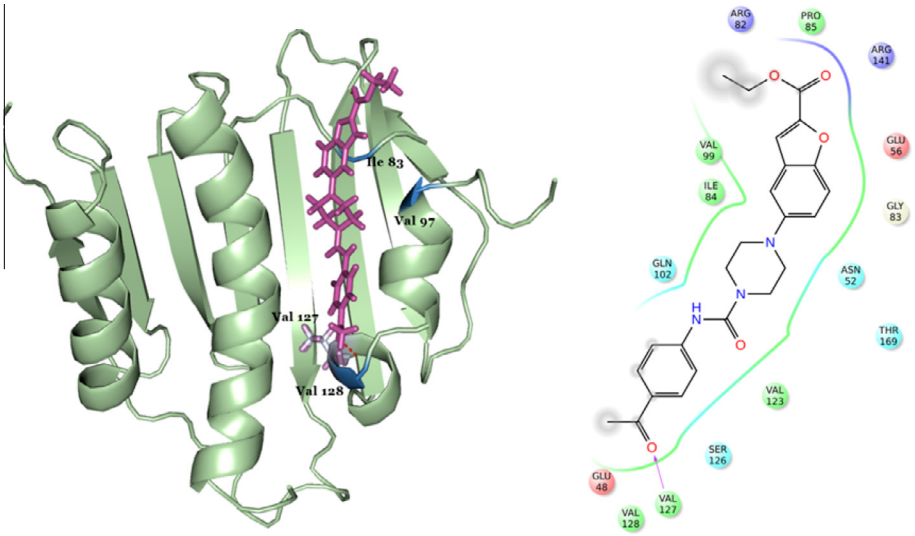

Figure 5. Interaction pattern of the compound **27** (*N*-(4-acetylphenyl)-4-(benzo[*d*]isothiazol-3-yl)piperazine-1-carboxamide) with GyrB ATPase domain of *M. smegmatis*. Hydrophobic pocket is represented by the blue color residues. No polar contacts are seen.

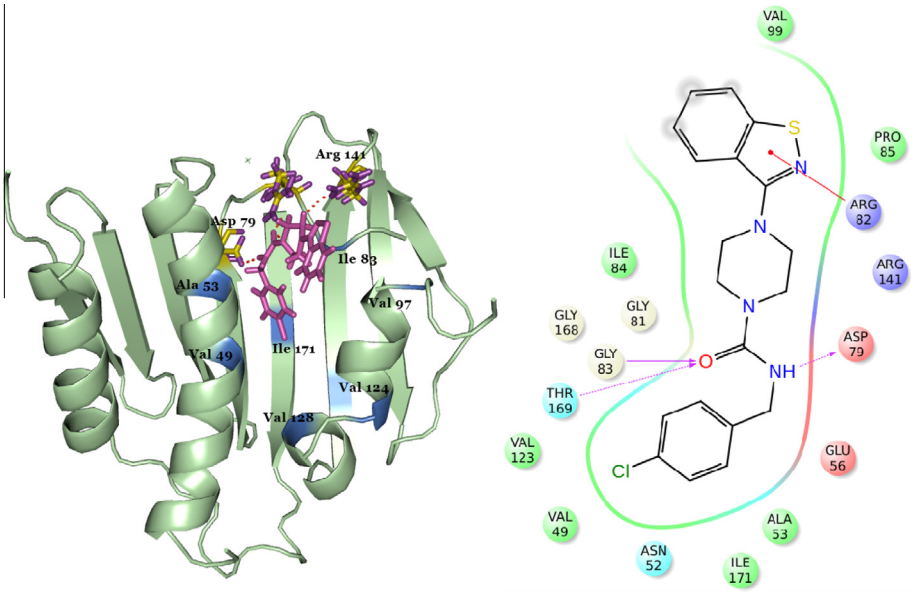

Figure 6. Interaction pattern of the compound **15** (ethyl 5-(4-(4-chlorobenzylcarbamoyl)piperazin-1-yl)benzofuran-2-carboxylate) with GyrB ATPase domain of *M. smegmatis*. Hydrophobic pocket is represented by the blue color residues and the polar contacts are shown by the red dotted lines.

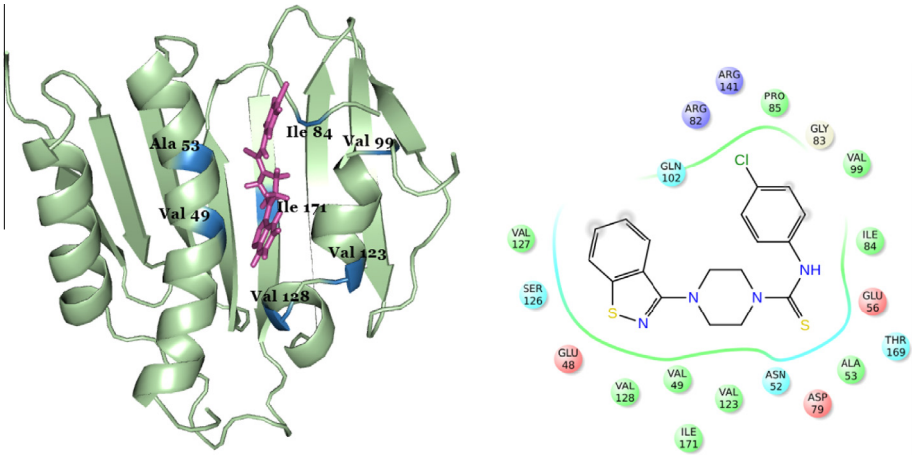

Figure 7. Interaction pattern of the compound **17** (ethyl 5-(4-(4-chlorophenylthiocarbamoyl)piperazin-1-yl)benzofuran-2-carboxylate) with GyrB ATPase domain of *M. smegmatis*. Hydrophobic pocket is represented by the blue color residues. No polar contacts are observed.

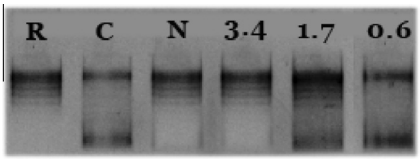

Figure 8. Depicting the supercoiling assay picture of compound **26** at three different concentrations of 3.4, 1.7, 0.6 μM, R-Relaxed DNA substrate + DMSO; C-Relaxed DNA substrate + DNA Gyrase + DMSO; *N*-novobiocin.

All the compounds were also tested for their ability to inhibit DNA supercoiling activity using MTB DNA gyrase supercoiling kit from Inspiralis (Inspiralis, Norwich). Each of the compounds tested showed dose-dependent inhibition of the mycobacterial gyrase enzyme. DNA supercoiling inhibition studies were done at an initial concentration of 50 μM, and almost twenty compounds out of twenty eight (**9**, **11**, **12**, **13**, **14**, **15**, **16**, **19**, **21**, **25**, **26**, **27**, **30**, **31**, **32**, **33**, **34**, **35**, **36** and **38**) showed more than 70% inhibition as depicted in Table 1. Further these compounds were tested for their inhibitions at lower concentrations to obtain IC_{50}, and the potent inhibitor **26** with good DNA GyrB inhibition also showed a better IC_{50} of 0.42 ± 0.23 μM in the supercoiling assay, while the standard compound novobiocin showed 100% inhibition at 50 and 25 μM with an IC_{50} of 46 ± 10 nM as illustrated in Figure 8. These compounds were target specific as they had not inhibited in *Escherichia coli*, *Staphylococcus aureus* and *Pseudomonas aeruginosa* DNA supercoiling assays (Inspiralis, Norwich).

Further in vitro antimycobacterial activity studies against *M. tuberculosis* H37Rv strain were performed by microplate Alamar blue assay method for all the twenty eight synthesized compounds.[15] Sixteen compounds (**10**, **12**, **13**, **17**, **20**, **26**, **29**, **30**, **31**, **32**, **33**, **34**, **35**, **36**, **37** and **38**) showed commendable MIC values <20 μM. First-line TB drugs ethambutol (MIC: 15.31 μM) and isoniazid (MIC: 0.66 μM) were used as standards along with moxifloxacin (MIC: 1.2 μM) and novobiocin (MIC: >200 μM). Few of the inhibitors (**13**, **26**, **29**, **30**, **31**, **32**, **33**, **34**, **35**, **36**, **37** and **38**) showed more potency than the standard ethambutol highlighting the importance of these compounds as effective drugs against mycobacterial growth.

Eukaryotic cells safety profile of all the compounds were observed by testing their in vitro cytotoxicity against mouse macrophage RAW 264.7 cell line at 100 μM concentration, employing (4,5-dimethylthiazol-2-yl)-2,5-diphenyltetrazolium bromide (MTT) assay.[16] The most promising analog **26** displayed a good safety profile showing 20.2%. Percentage inhibitions of cells of the compounds are reported in Table.1.

The interaction profile of compound **26** to stabilize the protein was evaluated by measuring the fluorescence of a dye with native DNA GyrB protein and its protein–ligand complex.[15] Fluorescence was maximum when the protein was denatured completely; as a result the native protein T_m was observed to be 43 °C whereas the T_m of the protein- in complex with **26** was found to be 46.1 °C as shown in the Figure 9. A higher or positive shift of T_m signified a better stabilization of the protein–ligand complex, which further re-ascertained for the interaction of the compound with DNA GyrB protein.

3. Conclusion

This work described the design of 28 molecules by molecular hybridization, synthesis and biological evaluation of MTB DNA GyrB inhibition. This class of molecules targeted selectively the mycobacterial DNA gyrase enzyme with promising attributes of synthetic accessibility well defined SAR, and antitubercular activity, suggesting potential for the development of new class of MTB gyrase inhibitors. In addition, molecular modeling studies were performed to explain the importance of these compounds and the orientation of various substituted side chains for their interactions with the enzyme active site. Furthermore, in this class of molecules the substituents at 4th position were attempted, substitutions at other positions would provide an interesting potential for further optimization.

4. Experimental section

4.1. Chemistry

Melting points (mp) reported in this work were recorded in capillary tubes on an Elchem lab melting point apparatus and uncorrected. ^{1}H NMR and ^{13}C NMR were recorded either in Bruker 500 MHz and 400 MHz FT-NMR spectrometer with 5 mm PABBO BB-1H tubes. ^{1}H NMR spectra recorded using approximately 0.03 M solutions in $CDCl_3$ with TMS as internal reference. ^{13}C NMR spectra were recorded using approximately 0.05 M solutions

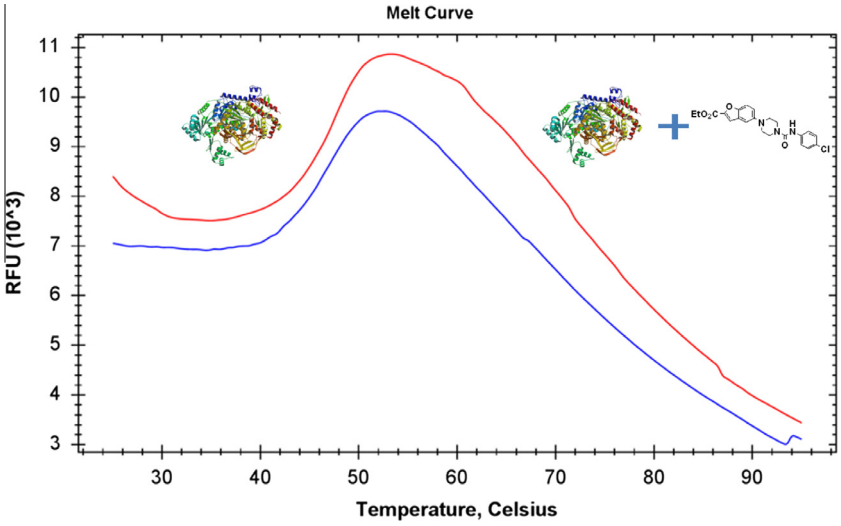

Figure 9. Melt curve for compound **26** showing an increase in thermal stability between the native MS DNA GyrB protein (red) and DNA GyrB protein–ligand **26** complex (blue) using differential scanning fluorimetry experiment.

in $CDCl_3$ at 100 MHz or 125 MHz with TMS as internal reference. The chemical shift values were reported in parts per million (δ, ppm) from internal standard TMS. Mass spectra were obtained from JEOL GC Mate HRMS analyzer. The UV–visible spectra were recorded on a SYSTRONIC AU-2701 UV–Vis spectrophotometer. All reagents were purchased from Aldrich and used as received. Solvents were removed under reduced pressure on a rotavapor. Organic extracts were dried with anhydrous Na_2SO_4. Silica gel $60F_{254}$ aluminum sheets were used in analytical thin-layer chromatography (TLC) and silica gel for column chromatography purification (230–400 mesh). Visualization of spots on TLC plates was effected by UV illumination, exposure to iodine vapor and heating the plates dipped in $KMnO_4$ stain.

4.1.1. Procedure for synthesis of 5-nitro salicylaldehyde (5)

Ethyl 5-nitro benzofuran-2-carboxylate (**6**), ethyl 5-amino benzofuran-2-carboxylate (**7**), ethyl 5-(piperazin-1-yl)benzofuran-2-carboxylate (**8**) were reported in Ref. 10.

4.1.2. General procedure for compounds (9–22) preparation

To the solution of ethyl 5-(piperazin-1-yl)benzofuran-2-carboxylate (1 mmol) in DCM, followed by addition of corresponding isocyanate (1.2 mmol) and stirred for 12 h at RT. To the RM added excess of DCM and wash with water. The organic layer was dried with Na_2SO_4 and evaporated to get the required compound.

4.1.3. Ethyl 5-(4-(phenylcarbamoyl) piperazin-1-yl)benzofuran-2-carboxylate (9)

Off white solid, yield (87%), mp: 311.5–312.9 °C, ^{1}H NMR (400 MHz, $CDCl_3$): δ = 8.18 (s, 1H), 7.26 (m, 6H), 6.39 (m, 1H), 4.42 (q, J = 7.2, 14.4 Hz, 2H), 3.71 (t, J = 5.2 Hz, 4H), 3.18 (t, J = 4.8 Hz, 4H), 1.41 (t, J = 7.2 Hz, 3H); ^{13}C NMR (300 MHz, DMSO+$CDCl_3$): 165.9, 159.0, 155.2, 150.7, 148.1, 145.6, 139.1, 128.3, 127.1, 122.3, 121.8, 120.0, 118.3, 113.3, 112.1, 108.4, 60.9, 50.4, 43.8, 13.9. MS calcd for $C_{22}H_{23}N_3O_4$: 393.4. Found: 394.6, (M^+); Anal. Calcd for $C_{22}H_{23}N_3O_4$: C, 67.16; H, 5.89; N, 10.68; Found: C, 67.17; H, 5.87; N, 10.71.

4.1.4. Ethyl 5-(4-(4-chlorophenylcarbamoyl)piperazin-1-yl) benzofuran-2-carboxylate (10)

Off white solid, yield (v), mp: 302.5–304.5 °C, ^{1}H NMR (400 MHz, $CDCl_3$): δ = 8.90 (s, 1H), 7.62 (m, 1H), 7.51 (m, 6H), 7.33 (m, 6H), 4.34 (q, J = 7.2, 14.4 Hz, 2H), 3.63 (t, J = 5.2 Hz, 4H), 3.15 (t, J = 4.8 Hz, 4H), 1.34 (t, J = 7.2 Hz, 3H); ^{13}C NMR (300 MHz, DMSO+$CDCl_3$): 163.0, 155.1, 152.2, 138.2, 127.9, 127.3, 126.7, 123.7, 123.2, 121.1, 120.1, 119.4, 49.9, 43.4. MS calcd for $C_{22}H_{22}ClN_3O_4$: 427.8. Found: 428.6, (M^+); Anal. Calcd for $C_{22}H_{22}ClN_3O_4$: C, 61.75; H, 5.18; N, 9.82. Found: C, 61.77; H, 5.15; N, 9.83.

4.1.5. Ethyl 5-(4-(4-acetylphenylcarbamoyl)piperazin-1-yl) benzofuran-2-carboxylate (11)

White solid, yield (93%), mp: 296.5–98.41 °C, ^{1}H NMR (400 MHz, $CDCl_3$): δ = 7.49 (d, J = 9.2 Hz, 1H), 7.44 (m, 4H), 7.12 (m, 2H), 7.12 (m, 1H), 4.89 (d, J = 5.2 Hz, 2H), 4.43 (q, J = 7.2, 14.4 Hz, 2H), 4.04 (t, J = 5.2 Hz, 4H), 3.25 (t, J = 5.2 Hz, 4H), 2.42 (s, 3H), 1.42 (t, J = 7.2 Hz, 3H); ^{13}C NMR (100 MHz, DMSO+$CDCl_3$): 195.6, 194.8, 153.9, 151.8, 147.4, 144.2, 129.6, 128.2, 127.6, 126.4, 119.2, 117.6, 112.1, 111.4, 107.8, 66.8, 60.2, 49.7, 45.1, 43.2, 29.2, 27.7, 25.3, 24.9, 21.8, 13.0. MS calcd for $C_{24}H_{25}N_3O_5$: 435.4. Found: 436.2, (M^+); Anal. Calcd for $C_{24}H_{25}N_3O_5$: C, 66.19; H, 5.79; N, 9.65; Found: C, 66.17; H, 5.82; N, 9.66.

4.1.6. 5-[4-(4-Nitro-phenylcarbamoyl)-piperazin-1-yl]-benzofuran-2-carboxylic acid ethyl ester (12)

White solid, yield (91%), mp: 268.9–269.1 °C, ^{1}H NMR (400 MHz, $CDCl_3$): δ = 8.20 (d, J = 9.2 Hz, 1H), 8.07 (m, 3H), 7.52 (m, 2H), 6.62 (m, 3H), 4.43 (q, J = 7.2, 14.4 Hz, 2H), 3.74 (t, J = 5.2 Hz, 4H), 3.23 (t, J = 4.8 Hz, 4H), 1.42 (t, J = 7.2 Hz, 3H); ^{13}C NMR (300 MHz, DMSO+$CDCl_3$): 181.4, 157.3, 155.2, 148.4, 144.6, 142.8, 129.6, 126, 122.2, 115.9, 111.5, 107.2, 59.8, 48.9, 48.2, 13.5. MS calcd for $C_{22}H_{22}N_4O_6$: 438.4. Found: 439.6, (M^+); Anal. Calcd for $C_{22}H_{22}N_4O_6$: C, 60.27; H, 5.06; N, 12.78; Found: C, 60.29; H, 5.05; N, 12.79.

4.1.7. Ethyl 5-(4-(4-methoxyphenylcarbamoyl)piperazin-1-yl) benzofuran-2-carboxylate (13)

White solid, yield (93%), mp: 297.5–299.4 °C, ^{1}H NMR (400 MHz, $CDCl_3$): δ = 7.51 (d, J = 8.8 Hz, 1H), 7.45 (s, 1H), 7.27 (m, 2H), 7.19 (m, 2H), 6.85 (d, J = 8.4 Hz, 2H), 6.32 (b, 1H), 4.43 (q, J = 7.2, 14.4 Hz, 2H), 3.78 (s, 3H), 3.69 (m, 4H), 3.21 (m, 4H), 1.42 (t, J = 7.2 Hz, 3H); ^{13}C NMR (100 MHz, DMSO+$CDCl_3$): 181.2, 158.6, 155.2, 154.6, 150.3, 147.6, 145.2, 132.1, 126.7, 121.8, 119.5, 113.0, 112.9, 111.7, 108.2, 60.5, 54.6, 50.2, 43.3, 13.5. MS calcd for $C_{23}H_{25}N_3O_5$: 423.4. Found: 424.5, (M^+). Anal. Calcd for $C_{23}H_{25}N_3O_5$: C, 65.24; H, 5.95; N, 9.92; Found: C, 65.25; H, 5.93; N, 9.94.

4.1.8. Ethyl 5-(4-(benzylcarbamoyl)piperazin-1-yl)benzofuran-2-carboxylate (14)

Off white solid, yield (88%), mp: 298.5–300.1 °C, ^{1}H NMR (400 MHz, $CDCl_3$): δ = 7.48 (m, 1H), 7.31 (m, 4H), 7.13 (m, 1H), 4.79 (b, 1H), 4.43 (q, J = 7.2, 14.4 Hz, 2H), 3.58 (t, J = 4.8 Hz, 4H), 3.15 (t, J = 5.2 Hz, 4H), 1.42 (t, J = 7.2 Hz, 3H); ^{13}C NMR (300 MHz, DMSO+$CDCl_3$): 181.2, 158.4, 157.9, 157.1, 150.0, 147.8, 145.0, 139.5, 119.4, 112.9, 111.5, 107.8, 62.3, 60.4, 49.9, 43.0, 24.5, 13.4. MS calcd for $C_{23}H_{25}N_3O_4$: 407.4. Found: 408.6, (M^+); Anal. Calcd for $C_{23}H_{25}N_3O_4$: C, 67.80; H, 6.18; N, 10.31; Found: C, 67.82; H, 6.17; N, 10.33.

4.1.9. Ethyl 5-(4-(4-chlorobenzylcarbamoyl)piperazin-1-yl) benzofuran-2-carboxylate (15)

White solid, yield (91%), mp: 285.5–286.4 °C, ^{1}H NMR (400 MHz, $CDCl_3$): δ = 7.28 (m, 6H), 4.43 (q, J = 7.2, 14.4 Hz, 2H), 4.14 (t, J = 5.2 Hz, 4H), 3.50 (m, 2H), 3.28 (m, 2H), 1.42 (t, J = 7.2 Hz, 3H); ^{13}C NMR (300 MHz, DMSO+$CDCl_3$): 181.6, 164.4, 158.5, 154.7, 151.3, 147.3, 136.3, 129.3, 126.4, 124.4, 122.3, 119.0, 115.5, 112.3, 111.1, 109.4, 59.9, 50.4, 48.9, 13.4. MS calcd for $C_{23}H_{24}ClN_3O_4$: 441.9. Found: 442.8, (M^+); Anal. Calcd for $C_{23}H_{24}ClN_3O_4$: C, 62.51; H, 5.47; Cl, 8.02; N, 9.51; Found: C, 62.53; H, 5.45; Cl, 8.01; N, 9.52.

4.1.10. Ethyl 5-(4-(phenylthiocarbamoyl)piperazin-1-yl) benzofuran-2-carboxylate (16)

Off white solid, yield (89%), mp: 276.7–277.9 °C, ^{1}H NMR (400 MHz, $CDCl_3$): δ = 7.49 (d, J = 8.8 Hz, 1H), 7.43 (d, J = 11.6 Hz, 2H), 7.35 (t, J = 7.6 Hz, 2H), 7.15 (m, 4H), 7.09 (m, 1H), 4.43 (q, J = 7.2, 14.4 Hz, 2H), 4.02 (t, J = 5.2 Hz, 4H), 3.23 (t, J = 4.8 Hz, 4H), 1.41 (t, J = 7.2 Hz, 3H); ^{13}C NMR (300 MHz, DMSO+$CDCl_3$): 182.4, 159.0, 150.6, 147.6, 145.7, 140.2, 128.1, 127.1, 124.7, 119.5, 113.3, 112.2, 108.2, 60.9, 49.9, 48.2, 13.9, 7.5. MS calcd for $C_{22}H_{23}N_3O_3S$: 409.5. Found: 410.4, (M^+). Anal. Calcd for $C_{22}H_{23}N_3O_3S$: C, 64.53; H, 5.66; N, 10.26; Found: C, 64.55; H, 5.64; N, 10.25.

4.1.11. Ethyl 5-(4-(4-chlorophenylthiocarbamoyl)piperazin-1-yl) benzofuran-2-carboxylate (17)

White solid, yield (87%), mp: 310.5–312.4 °C, ^{1}H NMR (400 MHz, $CDCl_3$): δ = 7.50 (d, J = 7.0 Hz, 1H), 7.43 (s, 1H), 7.21 (m, 4H), 6.32 (b, 1H), 4.43 (q, J = 7.2, 14.4 Hz, 2H), 3.82 (m, 4H), 3.10 (m, 4H), 1.42 (t, J = 7.2 Hz, 3H); ^{13}C NMR (100 MHz, DMSO+$CDCl_3$): 181.9, 157.9, 147.5, 145.5, 150.7, 138.9, 129.7, 127.9, 127.0, 126.3, 119.4, 113.2, 112.1, 108.1, 60.8, 49.8, 47.9, 13.8. MS calcd for $C_{22}H_{22}ClN_3O_3S$: 443.9. Found: 444.8, (M^+). Anal.

Calcd for $C_{22}H_{22}ClN_3O_3S$: C, 59.52; H, 4.99; Cl, 7.99; N, 9.47; Found: C, 59.53; H, 4.98; Cl, 7.97; N, 9.49.

4.1.12. Ethyl 5-(4-(4-acetylphenylthiocarbamoyl)piperazin-1-yl)benzofuran-2-carboxylate (18)

White solid, yield (86%), mp: 255.5–257.6 °C, ^{1}H NMR (400 MHz, $CDCl_3$): δ = 9.70 (s, 1H), 7.90 (d, J = 16.4 Hz, 2H), 7.63 (m, 2H), 7.50 (d, J = 8.8 Hz, 2H), 7.32 (dd, J = 2.4, 6.4 Hz, 1H), 7.23 (d, J = 2.4, 1H), 4.45 (q, J = 7.2, 14.4 Hz, 2H), 4.08 (t, J = 5.2 Hz, 4H), 3.26 (t, J = 5.2 Hz, 4H), 3.26 (m, 4H), 2.54 (s, 3H), 1.33 (t, J = 7.2 Hz, 3H); ^{13}C NMR (300 MHz, DMSO+$CDCl_3$): 182.6, 162.4, 154.4, 145.6, 142.6, 140.4, 129.8, 124.9, 123.1, 118.3, 113.8, 111.1, 109.4, 60.5, 49.8, 49.4, 13.9. MS calcd for $C_{24}H_{25}N_3O_4S$: 451.5. Found: 452.3, (M^+); Anal. Calcd for $C_{24}H_{25}N_3O_4S$: C, 63.84; H, 5.58; N, 9.31; Found: C, 63.85; H, 5.56; N, 9.33.

4.1.13. 5-[4-(4-Nitro-phenylthiocarbamoyl)-piperazin-1-yl]-benzofuran-2-carboxylic acid ethyl ester (19)

Yellow solid, yield (90%), mp: 310.5–312.4 °C, ^{1}H NMR (400 MHz, $CDCl_3$): δ = 8.39 (b, 1H), 8.18 (d, J = 8.8 Hz, 1H), 7.52 (m, 2H), 7.34 (s, 1H), 7.13 (m, 1H), 4.43 (q, J = 7.2, 14.4 Hz, 2H), 4.14 (t, J = 5.2 Hz, 4H), 3.50 (m, 2H), 3.28 (m, 2H), 1.42 (t, J = 7.2 Hz, 3H); ^{13}C NMR (100 MHz, DMSO+$CDCl_3$): 168.9, 158.6, 154.8, 152.8, 150.1, 144.2, 143.9, 133.5, 124.2, 123.8, 119.4, 113.5, 112.3, 101.6, 60.5, 53.9, 49.6, 42.3, 13.4. MS calcd for $C_{22}H_{23}N_4O_5S$: 455.5. Found: 456.6, (M^+); Anal. Calcd for $C_{22}H_{23}N_4O_5S$: C, 58.14; H, 4.88; N, 12.33; Found: C, 58.16; H, 4.87; N, 12.34.

4.1.14. Ethyl 5-(4-(4-methoxyphenylthiocarbamoyl)piperazin-1-yl)benzofuran-2-carboxylate (20)

White solid, yield (84%), mp: 254.5–256.4 °C, ^{1}H NMR (400 MHz, $CDCl_3$): δ = 7.50 (d, J = 9.2 Hz, 1H), 7.44 (s, 1H), 7.25 (s, 1H), 7.12 (m, 4H), 6.89 (d, J = 8.8 Hz, 2H), 4.43 (q, J = 7.2, 14.4 Hz, 2H), 4.03 (t, J = 4.8 Hz, 4H), 3.80 (s, 3H), 3.23 (t, J = 4.8 Hz, 4H), 1.34 (t, J = 7.2 Hz, 3H); ^{13}C NMR (300 MHz, DMSO+$CDCl_3$): 182.4, 162.0, 155.7, 145.9, 142.1, 141.8, 129.5, 126.4, 122.1, 116.2, 11262, 109.6, 59.9, 49.9, 48.6, 13.5. MS calcd for $C_{23}H_{25}N_3O_4S$: 439.5. Found: 440.6, (M^+); Anal. Calcd for $C_{23}H_{25}N_3O_4S$: C, 62.85; H, 5.73; N, 9.56; Found: C, 62.86; H, 5.75; N, 9.54.

4.1.15. Ethyl 5-(4-(benzylthiocarbamoyl)piperazin-1-yl)benzofuran-2-carboxylate (21)

White solid, yield (91%), mp: 284.2–286.5 °C, ^{1}H NMR (400 MHz, $CDCl_3$): δ = 7.49 (d, J = 9.2 Hz, 1H), 7.44 (m, 5H), 7.12 (m, 3H), 5.85 (b, 1H), 4.89 (d, J = 5.2 Hz, 2H), 4.43 (q, J = 7.2, 14.4 Hz, 2H), 4.04 (t, J = 5.2 Hz, 4H), 3.25 (t, J = 5.2 Hz, 4H), 1.42 (t, J = 7.2 Hz, 3H); ^{13}C NMR (100 MHz, DMSO+$CDCl_3$): 181.6, 157.2, 154.2, 153.8, 151.6, 147.8, 142.4, 134.1, 126.2, 120.2, 118.1, 113.9, 102.9, 101.2, 59.5, 54.6, 50.6, 42.3, 13.5. MS calcd for $C_{23}H_{25}N_3O_3S$: 423.5. Found: 424.6, (M^+). Anal. Calcd for $C_{23}H_{25}N_3O_3S$: C, 65.23; H, 5.95; N, 9.92; Found: C, 65.25; H, 5.93; N, 9.94.

4.1.16. Ethyl 5-(4-(4-chlorobenzylthiocarbamoyl)piperazin-1-yl)benzofuran-2-carboxylate (22)

Off white solid, yield (91%), mp: 297.5–299.4 °C, ^{1}H NMR (400 MHz, $CDCl_3$): δ = 7.49 (d, J = 9.2 Hz, 1H), 7.44 (s, 1H), 7.31 (m, 4H), 7.12 (m, 2H), 5.85 (s, 1H), 4.89 (d, J = 5.2 Hz, 2H), 4.43 (q, J = 7.2, 14.4 Hz, 2H), 4.04 (t, J = 5.2 Hz, 4H), 3.25 (t, J = 5.2 Hz, 4H), 1.42 (t, J = 7.2 Hz, 3H); ^{13}C NMR (100 MHz, DMSO+$CDCl_3$): 181.6, 158.5, 150.1, 147.3, 145.2, 137.2, 131.5, 128.3, 127.5, 126.7, 119.0, 113.0, 111.7, 107.7, 60.5, 49.5, 47.8, 46.9, 24.6, 13.5. MS calcd for $C_{23}H_{24}ClN_3O_3S$: 457.9. Found: 458.6, (M^+); Anal. Calcd for $C_{23}H_{24}ClN_3O_3S$: C, 60.32; H, 5.28; Cl, 7.74; N, 9.18; Found: C, 60.31; H, 5.29; Cl, 7.76; N, 9.21.

4.1.17. General procedure for synthesis of 3-(piperazin-1-yl) benzo[*d*]isothiazole

The compound 3-chloro-1, 2-benzisothiazole (1 mmol) was allowed to react with piperazine (1.2 mmol) in Ethanol at 80 °C for 36 h. Then reaction mixture was concentrate and RM was dissolved in ethyl acetate and washed with water. Ethylacetate layer dried with Na_2SO_4 and concentrate them and get 3-(piperazin-1-yl)benzo[*d*]isothiazole. White solid, 85% yield, mp 215–217 °C, ^{1}H NMR (400 MHz, $CDCl_3$): δ = 7.42 (t, J = 7.2 Hz, 1H), 7.29 (m, 3H), 4.14 (t, J = 4.8 Hz, 4H), 3.15 (t, J = 4.8 Hz, 4H); ^{13}C NMR (100 MHz, DMSO+$CDCl_3$): 166.8, 156.2, 135.8, 128.5, 127.6, 125.2, 124.9, 119.8, 53.6, 49.2, 46.6, 45.1, 7.1. MS calcd for $C_{19}H_{20}N_4OS_2$: 219.31. Found: 220.33, (M^+); Anal. Calcd for $C_{19}H_{20}N_4OS_2$: C, 60.24; H, 5.97; N, 19.16; S, 14.62; Found: C, 60.25; H, 5.99; N, 19.13; S, 14.61.

4.1.18. General procedure for compounds (23–38) preparation

To the solution of 3-(piperazin-1-yl)benzo[*d*]isothiazole (1 mmol) in DCM, followed by addition of corresponding isocyanates (1.2 mmol) or isothiocyanates (1.2 mmol) and stirred for 12 h at RT. To the RM excess of DCM was added and washed with water. The organic layer was dried with Na_2SO_4 and evaporated, to get the required compound.

4.1.19. 4-(Benzo[*d*]isothiazol-3-yl)-*N*-phenylpiperazine-1-carboxamide (25)

Off white solid, yield (85%), mp: 254.4–256.1 °C, ^{1}H NMR (400 MHz, $CDCl_3$): δ = 7.93 (d, J = 8.0, Hz, 1H), 7.84 (d, J = 8.0, Hz, 1H), 7.50 (t, J = 7.2, Hz, 1H), 7.39 (m, 3H), 7.31 (t, J = 7.6, Hz, 2H), 7.06 (t, J = 7.6, Hz, 1H), 3.74 (m, 4H), 3.60 (m, 4H), ^{13}C NMR (100 MHz, DMSO+$CDCl_3$): 163.3, 155.1, 152.0, 140.4, 128.3, 127.9, 127.3, 124.4, 124.1, 121.7, 121.0, 119.6, 49.5, 43.6, 7.1. MS calcd for $C_{18}H_{18}N_4OS$: 338.4. Found: 339.6, (M^+); Anal. Calcd for $C_{18}H_{18}N_4OS$: C, 63.88; H, 5.36; N, 16.56; Found: C, 63.89; H, 5.38; N, 16.54.

4.1.20. 4-(Benzo[*d*]isothiazol-3-yl)-*N*-(4-chlorophenyl) piperazine-1-carboxamide (26)

White solid, yield (86%), mp: 254.2–256.4 °C, ^{1}H NMR (400 MHz, $CDCl_3$): δ = 7.90 (dd, J = 8.0, 20.4 Hz, 2H), 7.51 (t, J = 6.8 Hz, 1H), 7.38 (m, 3H), 7.27 (m, 2H), 6.47 (s, 1H), 3.47 (m, 4H), 3.62 (m, 4H), ^{13}C NMR (100 MHz, DMSO+$CDCl_3$): 181.6, 162.2, 151.0, 143.5, 133.2, 129.5, 127.6, 125.1, 124.5, 122.6, 121.0, 51.9, 49.9, 48.7, 26.4, 7.0. MS calcd for $C_{18}H_{17}ClN_4OS$: 372.8. Found: 373.6, (M^+); Anal. Calcd for $C_{18}H_{17}ClN_4OS$: C, 57.98; H, 4.60; Cl, 9.51; N, 15.03; Found: C, 57.99; H, 4.61; N, 15.01.

4.1.21. *N*-(4-Acetylphenyl)-4-(benzo[*d*]isothiazol-3-yl) piperazine-1-carboxamide (27)

White solid, yield (91%), mp: 188.5–189.4 °C, ^{1}H NMR (400 MHz, $CDCl_3$): δ = 8.03 (dd, J = 8.4, 22.8 Hz, 2H), 7.85 (m, 2H), 7.59 (m, 1H), 7.32 (m, 3H), 4.14 (t, J = 4.8 Hz, 4H), 3.80 (t, J = 4.8 Hz, 4H), 2.54 (s, 3H), ^{13}C NMR (100 MHz, DMSO+$CDCl_3$): 182.5, 163.8, 155.4, 153.5, 132.8, 125.9, 123.6, 121.2, 120.4, 119.2, 118.0, 113.2, 55.1, 49.9, 47.8, 7.0. MS calcd for $C_{20}H_20N_4O_2S$: 380.4. Found: 381.2, (M^+); Anal. Calcd for $C_{20}H_20N_4O_2S$: C, 63.14; H, 5.30; N, 14.73; Found: C, 63.15; H, 5.29; N, 14.75.

4.1.22. 4-Benzo[*d*]isothiazol-3-yl-piperazine-1-carbothioic acid (4-nitro-phenyl)-amide (28)

White solid, yield (93%), mp: 254.3–255.4 °C, ^{1}H NMR (400 MHz, $CDCl_3$): δ = 8.15 (m, 4H), 7.57 (m, 4H), 4.16 (m, 4H), 3.61 (m, 4H), ^{13}C NMR (100 MHz, DMSO+$CDCl_3$): 181.0, 162.7, 152.0, 147.8, 142.0, 127.9, 127.1, 124.4, 124.2, 123.9, 122.4, 121.0, 51.9, 48.9, 48.2, 46.8, 42.8, 7.1. MS calcd for $C_{18}H_{18}N_5O_2S_2$:

400.5. Found: 401.3, (M^+); Anal. Calcd for $C_{18}H_{18}N_5O_2S_2$: C, 54.12; H, 4.29; N, 17.53; Found: C, 54.14; H, 4.27; N, 17.51.

4.1.23. 4-(Benzo[*d*]isothiazol-3-yl)-*N*-(4-methoxyphenyl) piperazine-1-carboxamide (29)

Brown solid, yield (91%), mp: 236.4–238.8 °C, ^{1}H NMR (400 MHz, $CDCl_3$): δ = 7.88 (dd, J = 8.0, 16.8 Hz, 2H), 7.56 (t, J = 6.8 Hz, 1H), 7.42 (t, J = 7.0 Hz, 1H), 7.20 (m, 2H), 6.90 (d, J = 7.2 Hz, 2H), 4.08 (t, J = 5.2 Hz, 4H), 3.80 (s, 3H), 3.66 (t, J = 5.2 Hz, 4H), ^{13}C NMR (100 MHz, DMSO+$CDCl_3$): 162.9, 155.5, 154.7, 151.9, 127.1, 123.5, 123.1, 122.0, 119.9, 113.0, 62.2, 54.7, 51.9, 49.3, 46.1, 43.2, 42.1, 7.0. MS calcd for $C_{19}H_{20}N_4O_2S$: 368.4. Found: 369.5, (M^+); Anal. Calcd for $C_{19}H_{20}N_4O_2S$: C, 61.94; H, 5.47; N, 15.21; Found: C, 61.96; H, 5.45; N, 15.22.

4.1.24. 4-(Benzo[*d*]isothiazol-3-yl)-*N*-benzylpiperazine-1-carboxamide (30)

Off white solid, yield (94%), mp: 187.5–189.4 °C, ^{1}H NMR (400 MHz, $CDCl_3$): δ = 7.91 (d, J = 8.4, 1H), 7.83 (d, J = 8.4, 1H), 7.48 (t, J = 6.8 Hz, 1H), 7.35 (m, 6H), 4.83 (b, 1H), 4.48 (t, J = 7.2 Hz, 2H), 3.61 (m, 8H), ^{13}C NMR (100 MHz, DMSO+$CDCl_3$): 163.4, 157.6, 152.7, 139.2, 128.5, 127.7, 127.6, 127.2, 124.0, 123.6, 120.5, 52.7, 49.6, 44.9, 43.5, 7.9. MS calcd for $C_{19}H_{20}N_4OS$: 352.4. Found: 353.6, (M^+); Anal. Calcd for $C_{19}H_{20}N_4OS$: C, 64.75; H, 5.72; N, 15.90; Found: C, 64.77; H, 5.70; N, 15.91.

4.1.25. *N*-(4-Chlorobenzyl)-4-(benzo[*d*]isothiazol-3-yl) piperazine-1-carboxamide (31)

White solid, yield (93%), mp: 199.5–201.6 °C, ^{1}H NMR (400 MHz, $CDCl_3$): δ = 7.89 (d, J = 8.0, Hz, 1H), 7.83 (d, J = 8.0, Hz, 1H), 7.51 (t, J = 7.6, Hz, 1H), 7.40 (t, J = 8.4, Hz, 1H), 7.30 (m, 4H), 4.84 (b, 1H), 4.44 (d, J = 5.6 Hz, 2H), 3.60 (m, 8H), ^{13}C NMR (100 MHz, DMSO+$CDCl_3$): 163.1, 157.5, 152.7, 137.9, 133.0, 129.0, 128.7, 127.7, 127.7, 124.1, 123.6, 120.6, 49.6, 44.2, 43.5, 8.0. MS calcd for $C_{19}H_{19}ClN_4OS$: 386.9. Found: 387.8, (M^+); Anal. Calcd for $C_{19}H_{19}ClN_4OS$: C, 58.98; H, 4.95; Cl, 9.16; N, 14.48; Found: C, 58.97; H, 4.97; N, 14.47.

4.1.26. 4-(Benzo[*d*]isothiazol-3-yl)-*N*-phenylpiperazine-1-carbothioamide (32)

White solid, yield (91%), mp: 198.6–200.4 °C, ^{1}H NMR (400 MHz, $CDCl_3$): δ = 7.87 (dd, J = 8.0, 14.8 Hz, 2H), 7.49 (m, 3H), 7.35 (m, 3H), 7.16 (m, 3H), 4.07 (t, J = 5.2 Hz, 4H), 3.65 (t, J = 5.2 Hz, 4H), ^{13}C NMR (100 MHz, DMSO+$CDCl_3$): 181.8, 162.9, 152.0, 141.0, 128.0, 127.2, 125.1, 124.4, 124.3, 124.2, 121.0, 99.3, 52.0, 49.0, 47.7, 46.6, 7.1. MS calcd for $C_{18}H_{18}N_4S_2$: 354.4. Found: 355.1, (M^+); Anal. Calcd for $C_{18}H_{18}N_4S_2$: C, 60.99; H, 5.12; N, 15.80; Found: C, 60.98; H, 5.14; N, 15.78.

4.1.27. 4-(Benzo[*d*]isothiazol-3-yl)-*N*-(4-chlorophenyl)piperazine-1-carbothioamide (33)

White solid, 93% yield, mp 264.3–266.4 °C, ^{1}H NMR (400 MHz, $CDCl_3$): δ = 8.12 (dd, J = 8.0, 16.4 Hz, 2H), 7.62 (t, J = 8.0 Hz, 1H), 7.32 (m, 3H), 7.12 (m, 2H), 4.02 (t, J = 5.2 Hz, 4H), 3.52 (t, J = 4.8 Hz, 4H), ^{13}C NMR (100 MHz, DMSO+$CDCl_3$): 181.8, 162.4, 151.9, 139.0, 129.2, 127.6, 127.2, 126.4, 123.6, 123.2, 120.0, 51.8, 48.8, 47.4, 7.0. MS calcd for $C_{18}H_{17}ClN_4S_2$: 388.9. Found: 389.8, (M^+); Anal. Calcd for $C_{18}H_{17}ClN_4S_2$: C, 55.59; H, 4.41; Cl, 9.12; N, 14.41; S, 16.49; Found: C, 55.61; H, 4.40; Cl, 9.13; N, 14.38; S, 16.50.

4.1.28. *N*-(4-Acetylphenyl)-4-(benzo[*d*]isothiazol-3-yl) piperazine-1-carbothioamide (34)

Off white solid, yield (94%), mp: 214.6–216.8 °C, ^{1}H NMR (400 MHz, $CDCl_3$): δ = 8.13 (dd, J = 8.4, 22.8 Hz, 2H), 7.91 (m, 2H), 7.60 (m, 1H), 7.49 (m, 3H), 4.14 (t, J = 4.8 Hz, 4H), 3.60 (t, J = 4.8 Hz, 4H), 2.54 (s, 3H), ^{13}C NMR (100 MHz, DMSO+$CDCl_3$): 196.6, 181.3, 162.8, 152.0, 145.6, 131.9, 128.5, 127.9, 127.1, 124.4, 124.2, 121.0, 51.9, 48.9, 48.0, 26.4, 7.1. MS calcd for $C_{20}H_{20}N_4OS_2$: 396.5. Found: 397.3, (M^+); Anal. Calcd for $C_{20}H_{20}N_4OS_2$: C, 60.58; H, 5.08; N, 14.13; Found: C, 60.59; H, 5.06; N, 14.15.

4.1.29. *N*-(4-Nitrophenyl)-4-(benzo[*d*]isothiazol-3-yl) piperazine-1-carbothioamide (35)

Off white solid, yield (89%), mp: 197.5–199.7 °C, ^{1}H NMR (400 MHz, $CDCl_3$): δ = 8.06 (m, 3H), 8.09 (d, J = 8.0 Hz, 1H), 7.75 (m, 2H), 7.58 (t, J = 8.0 Hz, 1H), 7.47 (t, J = 8.0 Hz, 1H), 3.74 (t, J = 4.4 Hz, 4H), 3.50 (t, J = 5.2 Hz, 4H), ^{13}C NMR (100 MHz, DMSO+$CDCl_3$): 163.2, 154.1, 152.0, 147.4, 145.6, 141.4, 140.8, 127.9, 127.2, 125.1, 124.6, 124.4, 124.1, 121.0, 118.3, 117.8, 51.9, 49.4, 43.7, 7.1. MS calcd for $C_{18}H_{18}N5O_3S$: 384.4. Found: 385.2, (M^+); Anal. Calcd for $C_{18}H_{18}N5O_3S$: C, 56.38; H, 4.47; N, 18.27; Found: C, 56.37; H, 4.45; N, 18.29.

4.1.30. 4-(Benzo[*d*]isothiazol-3-yl)-*N*-(4-methoxyphenyl) piperazine-1-carbothioamide (36)

White solid, yield (91%), mp: 185.5–186.4 °C, ^{1}H NMR (400 MHz, $CDCl_3$): δ = 7.88 (dd, J = 8.0, 16.8 Hz, 2H), 7.51 (t, J = 6.8 Hz, 1H), 7.40 (t, J = 8.4 Hz, 1H), 7.21 (m, 2H), 6.90 (d, J = 9.2 Hz, 2H), 4.08 (t, J = 5.2 Hz, 4H), 3.80 (s, 3H), 3.66 (t, J = 5.2 Hz, 4H), ^{13}C NMR (100 MHz, DMSO+$CDCl_3$): 182.0, 162.9, 156.4, 152.0, 133.8, 127.9, 127.3, 127.2, 124.4, 124.2, 121.0, 113.2, 55.1, 49.0, 47.5, 7.1. MS calcd for $C_{19}H_{20}N_4OS_2$: 384.5. Found: 385.6, (M^+); Anal. Calcd for $C_{19}H_{20}N_4OS_2$: C, 59.35; H, 5.24; N, 14.57; O, 4.16; Found: C, 59.37; H, 5.22; N, 14.58.

4.1.31. 4-(Benzo[*d*]isothiazol-3-yl)-*N*-benzylpiperazine-1-carbothioamide (37)

White solid, yield (90%), mp: 211.5–213.8 °C, ^{1}H NMR (400 MHz, $CDCl_3$): δ = 7.91 (d, J = 8.4 Hz, 1H), 7.83 (d, J = 8.4 Hz, 1H), 7.49 (m, 1H), 7.39 (m, 1H), 7.28 (m, 3H), 6.85 (m, 2H), 3.71 (m, 4H), 3.59 (m, 4H), ^{13}C NMR (100 MHz, DMSO+$CDCl_3$): 182.9, 162.6, 151.8, 151.4, 129.1, 123.3, 122.1, 122.0, 118.9, 111.6, 62.8, 53.9, 51.9, 48.3, 45.1, 43.7, 42.1, 7.0. MS calcd for $C_{19}H_{20}N_4S_2$: 368.5. Found: 369.6, (M^+); Anal. Calcd for $C_{19}H_{20}N_4S_2$: C, 61.92; H, 5.47; N, 15.20; Found: C, 61.94; H, 5.45; N, 15.22.

4.1.32. *N*-(4-Chlorobenzyl)-4-(benzo[*d*]isothiazol-3-yl) piperazine-1-carbothioamide (38)

Off white solid, yield (87%), mp: 235.5–237.48 °C, ^{1}H NMR (400 MHz, $CDCl_3$): δ = 7.89 (dd, J = 8.4, 21.6 Hz, 2H), 7.51 (m, 1H), 7.32 (m, 5H), 5.82 (s, 1H), 4.82 (s, 2H), 4.08 (m, 4H), 3.68 (m, 4H), ^{13}C NMR (100 MHz, DMSO+$CDCl_3$): 182.0, 162.9, 152.0, 138.7, 131.0, 129.0, 127.9, 127.9, 127.2, 124.4, 124.2, 121.0, 51.9, 48.9, 47.6, 47.0, 42.6, 7.1. MS calcd for $C_{19}H_{19}ClN_4S_2$: 402.9. Found: 403.8, (M^+); Anal. Calcd for $C_{19}H_{19}ClN_4S_2$: C, 56.63; H, 4.75; Cl, 8.80; N, 13.90; Found: C, 56.65; H, 4.74; N, 13.91.

4.2. Cloning and purification

In order to perform the ATPase assay MS GyrB protein was required. Subsequently, cloning of MS GyrB was done by amplifying the GyrB gene from the genomic DNA of mc2155 using specific forward and reverse primer with the sequence 5′ CACCCATATGGTGGCTGCC CAGAAGAACAA 3′ (NdeI), and 3′ AGCTAAGCTTTTAAACATCCAGGAAGCGAA 5′ (Hind III), respectively.[8] The final amplified PCR products were cloned in *E. coli* expression vector pQE2 (Qiagen) which was His-tagged and later was transformed into BL21 (DE3) pLysS cells. The transformed cells were grown at room temperature 37 °C in Luria Bertani (LB) broth containing 100 μg/mL ampicillin to an optical density (OD) of 0.5 (A595). Once bacterial cells reached an exponential growth phase,

they were induced with isopropyl-β-D-thiogalactopyranoside (IPTG) at a final concentration of 0.1 mM and the cell growth was further continued for another 12 h at 18 °C. Further, the bacterial cells were then centrifuged at 10,000 g and at 4 °C for 15 min. The cell pellet was resuspended in PBSG buffer (PBS containing 5% glycerol). Cells were then lysed using sonicator with (20 s pulse and 45 s halt) and centrifuged the crude lysate at 8000 rpm at 4 °C for 10 min; further centrifugation was repeated for the supernatant obtained from the previous step at 10,000 rpm at 4 °C for 45 min. The cell extract was later applied to Ni-NTA column (Bio-Rad). After washing the column with wash buffer (5% glycerol in PBS and 500 mM NaCl) desired protein was eluted using different concentration of imidazole ranging from 10 mM to 500 mM in the elution buffer (5% Glycerol, 140 mM NaCl in 25 mM Tris–Cl (pH 8.0)). Fractions containing the GyrB subunit were identified by running a sodium dodecyl sulfate–polyacrylamide gel electrophoresis (SDS–PAGE), samples were pooled; dialysed against 15% glycerol, 140 mM NaCl in 25 mM Tris–Cl (pH 7.4); frozen in liquid nitrogen and stored at −80 °C.

4.3. MS GyrB ATPase assay

The ATPase assay was performed in the presence of ATP molecule which got hydrolyzed similar to the previously reported protocol.[12] Briefly, the assay was carried out in 30 μL reaction volume for 2 h at 25 °C in reaction buffer containing 60 mM HEPES–KOH (pH 7.7), 250 mM potassium glutamate, 200 mM KCl, 2 mM magnesium chloride, 1 mM DTT, 2% Glycerol, 4% DMSO, 0.001% BriJ-35, 40 nM GyrB and 0.65 mM ATP. All the test compounds were diluted in DMSO to about 30 times the final assay concentration. Assay was performed in 96-well V-shape bottomed plates (Polystyrene untreated). Initially 1 μL of test compound was placed in the assay wells, which was followed by 15 μL of concentrated 2× assay buffer which includes 1 μL of purified GyrB enzyme and substrate mix, the enzyme reaction was initiated by adding 14 μL of 2 mM $MgCl_2$ solution. Then the reaction was allowed to proceed for 100 min at room temperature. Further, the reaction was quenched by adding 20 μL of malachite green reagent (Bioassay systems, USA). The inorganic phosphates (Pi) released after the reaction was measured at 635 nm after incubating for 20 min.

4.4. MTB DNA supercoiling assay

Supercoiling assay is performed by the A_2B_2 holoenzyme of DNA gyrase. The assay was performed using MTB DNA supercoiling assay kit (Inspiralis Limited, Norwich), in brief the assay was performed in 30 μL reaction volume for a period of 30 min at 37 °C in assay buffer containing 50 mM HEPES. KOH (pH 7.9), 6 mM magnesium acetate, 4 mM DTT, 1 mM ATP, 2 mM spermidine, 100 mM potassium glutamate, and 0.05 mg/mL of albumin. During the assay 1 U of MTB DNA gyrase was incubated with 0.5 μg of relaxed pBR322 substrate in 1× assay buffer. Later the reaction was quenched by the addition of equal volume of 30 μL of chloroform: isoamylalcohol (24:1) and STEB (40% sucrose, 100 mM Tris HCl (pH 8.0), 100 mM EDTA, 0.5 mg/mL bromophenol blue) subjected to a brief vortex, followed by centrifugation at 6000 rpm. The final product was analyzed by electrophoresis by running on 1% agarose gel and by staining with ethidium bromide (EtBr). Destaining was performed using Image lab software (Bio-Rad), intensity of the bands were measured and analyzed to know the enzyme inhibition by relative band intensity when compared to the positive control.

4.5. In vitro MTB MABA assay

To perform the MABA assay, the inoculum was prepared from fresh LJ medium, resuspended in 7H9 medium (7H9 broth, 0.1% casitone, 0.5% glycerol, supplemented oleic acid, albumin, dextrose, and catalase [OADC]), later adjusted to a McFarland tube No. 1, and diluted 1:20; further 100 μL was used as inoculums.[16] Each dissolved drug stock was thawed and diluted in 7H9-S at four-fold the final highest concentration tested. In this way, serial two-fold dilutions of each drug were prepared directly in a sterile 96 flat-bottomed well microtiter plate using 100 μL 7H9-S. A control containing no antibiotic and a sterile control were also prepared for each plate. In order to avoid evaporation of the contents during the incubation for 7 days, sterile water was added to all perimeter wells. The plate was covered with the lid, sealed in plastic bags and incubated at 37 °C at normal atmosphere. After seven days of incubation, 30 μL of Alamar blue solution was added to each well, and the plate was re-incubated overnight. A change in color from blue (oxidized state) to pink (reduced) indicated the growth of bacteria, and so the MIC was defined as the lowest concentration of drug that prevented this change in color.

4.6. In vitro cytotoxicity screening

The safety profile of all the compounds in the eukaryotic cells were examined by evaluating their in vitro cytotoxicity against mouse macrophages RAW 264.7 cell line at a concentration of 100 μM. After 72 h of exposure of the drug with the cells, viability was assessed on the basis of cellular conversion of the dye MTT into a formazan product using the Promega Cell Titer 96 non-radioactive cell proliferation assay.[17] The absorbance was read at 560 nm after 10 min incubation.

4.7. Differential Scanning fluorimetry (DSF)

The thermal stability of the protein with the ligand and affinity of most potent ligand with the protein of our interest can be known by using DSF technique. The assay was carried in 15 μL reaction volume consisting of 3.5 μL of assay buffer (50 mM Tris pH 7.4, 1 mM EDTA, 5 mM DTT), 7.5 μL of DNA gyrB protein (1.5 mg/mL) and 2.5 μL of Sypro orange dye (1:100) (Sigma) which were subjected to stepwise heating in a PCR instrument (Bio-Rad) from 25 °C to 100 °C with an increment of 0.6 °C/min.[18] With increase in temperature the protein, slowly unfolds and the inner hydrophobic residues get exposed, eventually more dye binds to the protein and fluorescence increases till it reaches equilibrium and this point is termed as melting temperature (T_m).[17] When the affinity of inhibitor is strong we observe a positive shift or increase in T_m when compared to the native protein T_m.

4.8. Molecular modelling studies

The most active compound which was proved to be active in MS DNA gyrB and MTB DNA supercoiling assay was docked onto the active pocket of the GyrB ATPase domain of MS retrieved from Protein Data Bank (PDB ID: 4B6C). The protein was initially processed (optimized and minimized) using the Protein Preparation Wizard of Schrödinger Suite 2012.[19] Further, the optimization of the hydrogen-bonding network and also the ligands to be docked were sketched in Maestro panel of Schrödinger and optimized with OPLS force field.[20] The docking of these molecules with the protein was done using Glide v5.8.[21]

Acknowledgment

D.S. would like to thank University Grant Commission, Government of India for UGC researcher award.

References and notes

1. Kale, M. G.; Raichurkar, A.; Waterson, S. H. P. D.; McKinney, D.; Manjunatha, M. R.; Koushik, K.; Jena, L. K.; Shinde, V.; Rudrapatna, S.; Barde, S.; Humnabadkar, V.; Madhavapeddi, P.; Basavarajappa, H.; Ghosh, A.; Ramya, V. K.; Guptha, S.; Sharma, S.; Vachaspati, P.; Kumar, K. N.; Giridhar, J.; Reddy, J.; Panduga, V.; Ganguly, S.; Ahuja, V.; Gaonkar, S.; Kumar, C. N.; Ogg, D.; Tucker, J. A.; Boriack-Sjodin, P. A.; de Sousa, S. M.; Sambandamurthy, V. K.; Ghorpade, S. R. *J. Med. Chem.* **2013**, *56*, 8834.
2. Aboul-Fadl, T.; Abdel-Aziz, H. A.; Abdel-Hamid, M. K.; Elsaman, T.; Thanassi, J.; Pucci, M. J. *Molecules* **2011**, *16*, 7864.
3. World Health Organization. Global Tuberculosis Control; WHO 2011 Report on Tuberculosis. http://www.who.int/mediacentre/news/releases/2011/tb_20111011/en/index.html.
4. World Health Organization. Multidrug and Extensively Drug-Resistant TB (M/XDR-TB); WHO 2010 Global Report on Surveillance and Response.
5. Cole, S. T.; Brosch, R.; Parkhill, J.; Garnier, T.; Churcher, C.; Harris, D.; Gordon, S. V.; Eiglmeier, K.; Gas, S.; Barry, C. E.; Tekaia, F.; Badcock, K.; Basham, D.; Brown, D.; Chillingworth, T.; Connor, R.; Davies, R.; Devlin, K.; Feltwell, T.; Gentles, S.; Hamlin, N.; Holroyd, S.; Hornsby, T.; Jagels, K.; Krogh, A.; McLean, J.; Moule, S.; Murphy, L.; Oliver, K.; Osborne, J.; Quail, M. A.; Rajandream, M. A.; Rogers, J.; Rutter, S.; Seeger, K.; Skelton, J.; Squares, R.; Squares, S.; Sulston, J. E.; Taylor, K.; Whitehead, S.; Barrell, B. G. *Nature* **1998**, *393*, 537.
6. Aubry, A.; Fisher, L. M.; Jarlier, V.; Cambau, E. *Biochem. Biophys. Res. Commun.* **2006**, *348*, 158.
7. Champoux, J. J. *Annu. Rev. Biochem.* **2001**, *70*, 369.
8. Jeankumar, V. U.; Renuka, J.; Santosh, P.; Soni, V.; Sridevi, J. P.; Suryadevara, P.; Yogeeswari, P.; Sriram, D. *Eur. J. Med. Chem.* **2013**, *70*, 143.
9. Kaur, P.; Agarwal, S.; Datta, S. *PLoS One* **2009**, *4*, e5923.
10. Renuka, J.; Reddy, K. I.; Srihari, K.; Jeankumar, V. U.; Shravan, M.; Sridevi, J. P.; Babu, K. S.; Yogeeswari, P.; Sriram, D. *Bioorg. Chem.* **2014**, *22*, 4924.
11. Stokes, N. R.; Thomaides-Brears, H. B.; Barker, S.; Bennett, J. M.; Berry, J.; Collins, I.; Czaplewski, L. G.; Gamble, V.; Lancett, P.; Logan, A.; Lunniss, C. J.; Peasley, H.; Pommier, S.; Price, D.; Smee, C.; Haydon, D. J. *Antimicrob. Agents Chemother.* **2013**, *57*, 5977.
12. Shirude, P. S.; Madhavapeddi, P.; Tucker, J. A.; Murugan, K.; Patil, V.; Basavarajappa, H.; Raichurkar, A. V.; Humnabadkar, V.; Hussein, S.; Sharma, S.; Ramya, V. K.; Narayan, C. B.; Balganesh, T. S.; Sambandamurthy, V. K. *ACS Chem. Biol.* **2013**, *8*, 519.
13. Friesner, R. A.; Murphy, R. B.; Repasky, M. P.; Frye, L. L.; Greenwood, J. R.; Halgren, T. A.; Sanschagrin, P. C.; Mainz, D. T. *J. Med. Chem.* **2006**, *49*, 6177.
14. Franzbalu, G. S.; Witzig, S. R.; McLaughlin, C. J.; Torres, P.; Madico, G.; Hernandez, A.; Degnan, T. M.; Cook, B. M.; Quenzer, K. V.; Ferguson, M. R.; Gilman, H. R. *J. Clin. Microbiol.* **1998**, *36*, 362.
15. Gerlier, D.; Thomasset, N. *Immunol. Methods* **1986**, *94*, 57.
16. Niesen, F. H.; Berglund, H.; Vedadi, M. *Nat. Prot.* **2007**, *2*, 2212.
17. Brvar, M.; Perdih, A.; Renko, M.; Anderluh, G.; Jerala, R.; Solmajer, T. *J. Med. Chem.* **2012**, *55*, 6413.
18. Brvar, M.; Perdih, A.; Hodnik, V.; Renko, M.; Anderluh Hodnik, G.; Renko, V.; Anderluh, M.; Jerala, G.; Solmajer, R.; Bioorg, T. *Med. Chem.* **2012**, *20*, 2572.
19. (a) *Protein Preparation Wizard*; Schrödinger Suite, 2012; (b) *Epik Version 2.2*; Schrödinger, LLC: New York, NY, 2012; (c) *Impact Version 5.7*; Schrödinger Suite: New York, NY, 2012; (d) *Prime Version 2.3*; Schrödinger Suite: New York, NY, 2012.
20. Kar, R. K.; Suryadevara, P.; Sahoo, B. R.; Sahoo, G. C.; Dikhit, M. R.; Das, P. *SAR QSAR Environ. Res.* **2013**, *24*, 215.
21. *Glide, Version 5.8*; Schrödinger, LLC: New York, NY, 2012.